Available online at www.sciencedirect.com
ScienceDirect
Journal of Cultural Heritage 9 (2008) 66–76
Journal of Cultural Heritage
http://france.elsevier.com/direct/CULHER/

Original article

Swelling damage in clay-rich sandstones used in the church of San Mateo in Tarifa (Spain)

Eduardo Sebastián [a], Giuseppe Cultrone [a,*], David Benavente [b], Lucia Linares Fernandez [c], Kerstin Elert [a], Carlos Rodriguez-Navarro [a]

[a] *Departamento de Mineralogía y Petrología, Facultad de Ciencias, Universidad de Granada, Fuentenueva s/n, 18002 Granada, Spain*
[b] *Laboratorio de Petrología Aplicada, Unidad Asociada CSIC-UA, Departamento de Ciencias de la Tierra y del Medio Ambiente, Universidad de Alicante, Apdo. 99, 03080 Alicante, Spain*
[c] *Departamento de Construcciones Arquitectónicas, Universidad de Alicante, 03000 Alicante, Spain*

Received 19 February 2007; accepted 12 September 2007

Abstract

This study shows that the sandstone used in the construction of the Church of San Mateo in Tarifa (Cádiz, Spain) is highly sensitive to processes of decay because of a combination of factors that are intrinsic and extrinsic to the material. The mineralogy, texture and porous system of the sandstone and the proximity of the church to the sea all play a part in these processes. X-ray diffraction reveals that there are interstratified chlorite/smectite clays among the minerals that make up the rock. These mixed layer clays have been shown to undergo hydric expansion. This phenomenon may be accompanied and augmented by the presence of NaCl which acts as an electrolyte in osmotic swelling processes. Two varieties of sandstone were used in the construction of the church, namely grey sandstone and brown sandstone. The latter is more porous and undergoes greater hydric expansion, showing a higher degree of deterioration. Ultrasound analysis has demonstrated that both varieties are anisotropic because they contain bedding planes and are affected by the preferred orientation of the phyllosilicates in the rock. The anisotropic nature of these stones was confirmed by capillary suction tests. The capillary front reaches a relatively low height which means that when water is absorbed, the anisotropic textural properties combined with the presence of chlorite–smectite mixed layers in the sandstone result in mechanical (shear) stress between the first few centimetres of the wet stone and the dry area behind. The latter effect favours the development of flakes, so causing the decay of the ornamental stone and the church façade.

Keywords: Sandstone decay; Clay minerals; Anisotropy; Hydric expansion; NaCl

1. Introduction and research aims

Historic monuments and buildings are subjected to a continuous process of decay over time which causes damage that is almost always irreparable [1]. In many cases the durability (as opposed to the alterability) of building materials is difficult to predict because of the large number of variables involved [2,3]. By isolating some of these variables we can focus our research on analysing the decay process and thereby design conservation methods that can halt the deterioration of historic buildings.

Most of the research on damage suffered by building stone has focused on chemical processes such as the effects of atmospheric pollution [4,5] or the dissolution of carbonate minerals [6–8], on certain aspects of physical decay such as salt crystallization [9] or problems of biodeterioration [10]. In contrast, relatively little has been published on the phenomena associated with hydric expansion [11,12]. Hydric expansion of a stone material is due in most cases to the presence of clay minerals. Clay minerals are common cementing materials in sandstone

* Corresponding author. Tel.: +34 958 240077; fax: +34 958 243368.
E-mail addresses: rolando@ugr.es (E. Sebastián), cultrone@ugr.es (G. Cultrone), david.benavente@ua.es (D. Benavente), lucia.linares@ua.es (L. Linares Fernandez), kelert@ugr.es (K. Elert), carlosrn@ugr.es (C. Rodriguez-Navarro).

1296-2074/$ - see front matter © 2007 Elsevier Masson SAS. All rights reserved.
doi:10.1016/j.culher.2007.09.002

used in buildings [13,14–16]. In fact, in Central Europe (in Germany, for example) clays typically appear as minor components in heavily decayed sandstone constructions [17].

The aggregation/disaggregation or swelling/shrinking of the clay particles occurs when these particles interact with water causing a whole series of identifiable pathologies in building stone [18]. A recent review of stone decay caused by the expansion of clays was published by Delgado Rodrigues [13] who proposed a way of measuring the durability of rocks by establishing an index of porosity, deformation by swelling and resistance to compression. Different clays react differently to hydric expansion, while the textural anisotropy of clay-bearing stones appears to play a critical role on swelling-shrinking related damage. Dunn and Hudec [19] have demonstrated that rocks with up to 30% of certain clay minerals homogeneously distributed along the stone matrix proved very resistant, while others in which clays were relatively minor constituents, but preferentially oriented along bedding planes, suffered serious damage. There is however very little information about the relationship between a homogeneous or anisotropic distribution of clays in a rock, its clay mineralogy, and its decay due to hydric expansion.

Clays exist in a wide variety of rocks either as primary (sedimentary rocks) or secondary components (magmatic and metamorphic rocks) [13]. Sandstone is a sedimentary rock with mineral phases that normally include clays. Research has shown that the presence of these clays can affect the durability of the stone [11,12,20–22].

The example presented in this article illustrates how different factors, including the presence of clays, may combine to produce serious decay in sandstone used in the construction of important monuments in Spain's Architectural Heritage.

One of the main objectives of our research was to identify the causes of selective decay in the case of the Church of San Mateo in Tarifa (Cádiz, Spain), which we believe would be a worthwhile contribution to any future restoration work and might be a representative example for understanding clay-related damage of building stones. Our study seeks to establish whether this decay was due to the intrinsic properties of the building material (mineralogy, texture) or to factors that were extrinsic to it (proximity of the church to the sea) or to a combination of both. We also investigated the relationship between the petrographic and physical characteristics of the stone and its response to hydric expansion.

2. Materials and methods

2.1. Church of San Mateo

The Church of San Mateo is located in the centre of the historic quarter of Tarifa (Cádiz, Spain) and is one of the town's principal monuments. The original structure in late Gothic style was begun at the beginning of the 16th Century and new parts were added in the 18th and 19th Centuries to complete the church as we know it today.

Our research centred on the Puerta del Perdón, the grand door of the main façade (south) known as the Fachada del Evangelio (Fig. 1) which, architecturally speaking, was built in the Baroque style, although it has some neoclassical decorative features.

Fig. 1. View of the Puerta del Perdón of the Church of San Mateo in Tarifa.

Three types of ornamental rock were used in the construction of this door: limestone, calcarenite and sandstone. The most widely used was sandstone which also showed the most severe signs of decay.

Two different types of sandstone were used; one was light brown and the other was of a darker, greyish colour. Both varieties suffered the same forms of decay but damage was more severe in the light brown stone.

This façade shows extensive crumbling and flaking [23]. The former typically involves the loss of large volumes of sandstone, especially in sheltered areas such as below the cornices (Fig. 2a). The stone loses fragments grain by grain due to a lack of interparticle cohesion. In some areas honeycombs are developed. In extreme situations hollows or small cavities appear. The flaking process normally involves the development of scales or flakes that are up to several centimetres long, which are detached from the underlying healthy stone (Fig. 2b).

In some places we observed flakes that follow the contour of the worked surface of the stone, a phenomenon known as "contour scaling" [24]. These flakes are normally several centimetres thick and when the process is well-advanced, the entire external layer is lost and the underlying rock is laid bare. This underlying rock is either extremely crumbly or shows serious scaling (Fig. 2c).

Some of the masonry work in sandstone also contains fissures. At an early stage in the decay process these materials have a fractured surface, almost as if they had "exploded" (Fig. 2d). If this process continues the fractures get deeper causing large amounts of stone to break off.

2.2. The ancient quarry

Most of the stone used in the building of the Church of San Mateo came from a quarry situated about two kilometres north-east of the town in the area known locally as the "Camino del Olivar". The quarry has a vertical work face, with

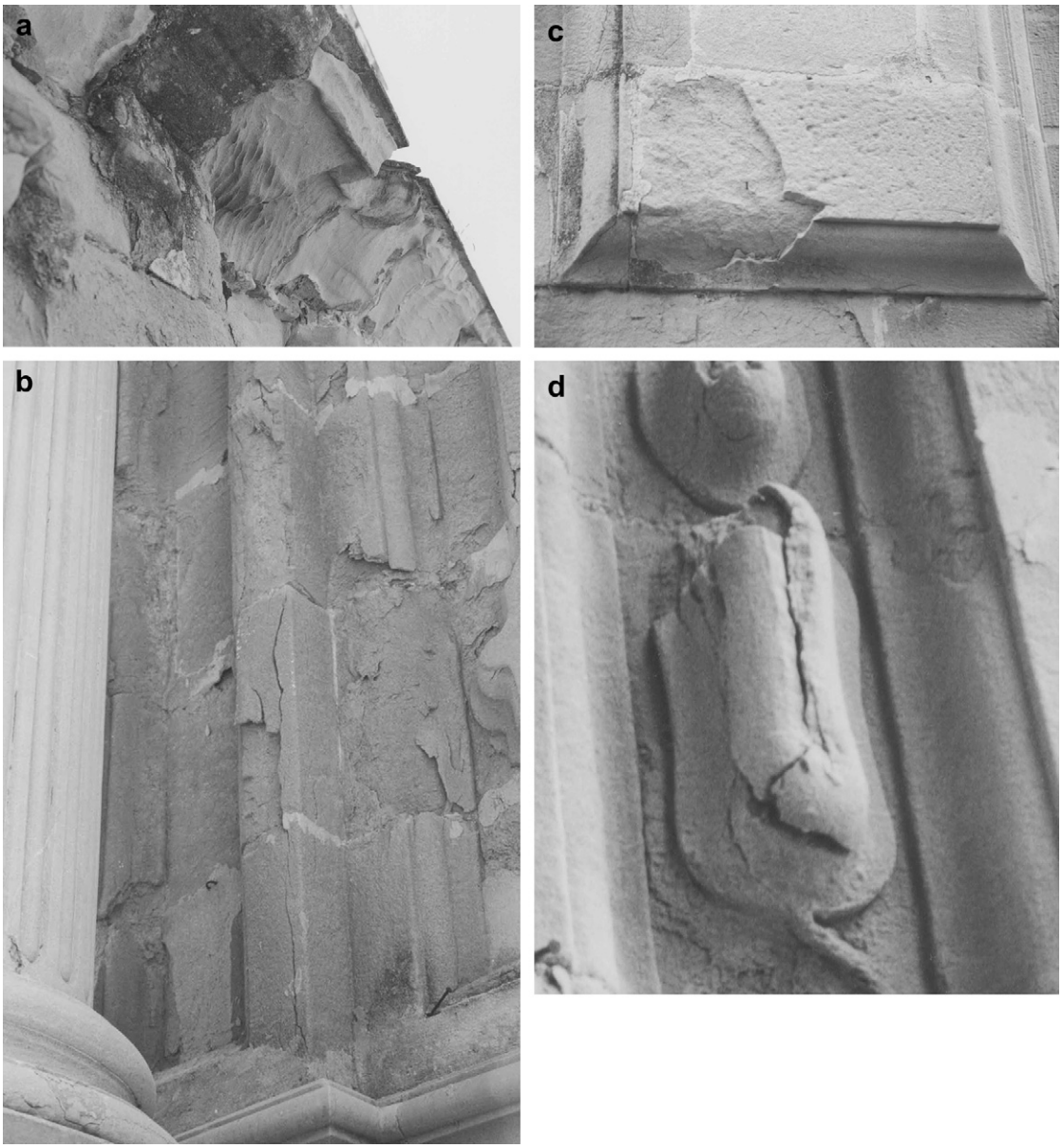

Fig. 2. Details of the Puerta del Perdón showing the high degree of decay of the sandstone: (a) crumbling; (b) flakes; (c) contour scaling; (d) fracturing.

a number of stepped levels which imply that it has been used until relatively recently. The sandstone is clearly visible in strata about 50 cm thick, which contain pronounced bedding planes that enabled the extraction of blocks with dimensions similar to those used in the ashlars of the church we are studying. With the naked eye, it is possible to distinguish the varieties used in the church: grey sandstone and brown sandstone. Geologically speaking, the sandstones belong to the Algeciras Unit of Oligocene-Aquitanian age [25]. This sequence is over 1000 m thick and contains micaceous, feldspatic and calcareous sandstones and marls [26]. These rocks may contain different combinations of clay minerals [27,28].

2.3. Samples and analysis

The samples used were either small fragments (broken off from the façade) of sandstone from the Puerta del Perdón or large blocks from the quarry used for the characterization of the stone. The mineralogical, petrographical and physical properties of the samples were studied. The samples from the Church of San Mateo were identified with the letter T and those from the quarry with TC.

X-ray diffraction (XRD) was employed to identify the mineralogical composition of the sandstone. A Philips PW 1710 diffractometer equipped with an automatic slit was used. The following conditions were applied: CuKα radiation, 40 kV, 40 mA, 3° to 60° 2θ explored area and 0.1° 2θ/s goniometer speed. The data were interpreted using the XPowder software package [29].

$\varnothing > 20$ μm, $2 < \varnothing < 20$ μm and $\varnothing < 2$ μm fractions were separated in order to determine any mineralogical differences between the different fractions and, at the same time, compare the mineralogy of the samples from the quarry with those from the church. The final aim of this analysis was to

verify if it was possible to recognize a mineral phase (or phases) that could have a negative effect on the durability of the sandstone.

Carbonates were eliminated using a 0.2 N acetic acid solution and the three fractions were separated using a Kubota 2000 centrifuge in the case of the <2 μm fraction, and the gravitational method (Stokes' Law) for the other two fractions [30].

Oriented aggregates of air dried (AO), solvated with ethylene-glycol at 60 °C for 48 h [31] (AO + EG), solvated with dimethyl-sulphoxide at 80 °C for 72 h [32] (AO + DMSO), and heated to 550 °C for 90 min [33] (AO + 550 °C) clay samples were prepared for XRD analysis.

The mineralogy and texture of sandstone samples was further examined using a polarized optical microscope (Olympus BX-60) and a scanning electron microscope (SEM) Zeiss DMS 950 coupled with Microanalysis Link QX 2000.

Elastic properties (the degree of compactness) of the samples from the quarry were studied using a Steinkamp BP5 ultrasonic pulse generator with 100 kHz transducers according to ASTM D 2845 [34]. Total anisotropy (ΔM) was determined using the mathematical formulae proposed by Guydader and Denis [35].

In order to assess the hydric behaviour of the stone from the quarry, absorption [36], absorption under vacuum [37,38], drying [39] and capillarity [40] tests were carried out on three test samples per variety of sandstone. The open porosity and the real and apparent density were calculated following the UNI EN 1936 [41] normative. The specimens used for absorption and drying tests were cubic in shape with a 4 cm edge, while those used for suction by capillarity were prism-shaped (2 × 3 × 3 cm). The prism-shape (not considered in standard test [42]) was selected to highlight the anisotropic behaviour during capillary suction in three perpendicular directions (number 1 corresponds to the direction of water capillary rise perpendicular to the bedding planes in the sandstone; and numbers 2 and 3 to the directions parallel to the bedding). The last two directions were considered in order to single out any linear preferred orientation of clay and/or quartz grains along bedding planes.

In order to measure the pore access size distribution and the open porosity of the sandstones from the church and from the quarry we used a Micromeritics AutoPore III 9410 mercury intrusion porosimeter (MIP). Three MIP measurements per sample were made. Nitrogen adsorption was used to complete the analysis of the micro and mesoporosity. Pore size distribution (PSD) in the range 0.0018–0.030 μm was obtained by N_2 adsorption (at 77 K) on an Autosorb-6 Quantachrome apparatus. PSD was calculated using the non-local density functional theory considering a silica pore model.

Finally, the hydric swelling of the rocks was characterized on prism-shaped specimens measuring 10 × 10 × 30 mm (longest direction normal to de bedding planes). The vertical deformation that occurred during the entry of water by capillarity in a direction perpendicular to the bedding plane was quantified with a Sensorex LVDT-SX8 displacement sensor (±1 μm resolution).

3. Results

3.1. Mineralogy

The sandstones from the Puerta del Perdón and from the quarry are practically identical from a mineralogical and textural point of view. This confirms that this quarry was indeed the source of the stone for the church. Its most abundant phase is quartz (70–85%), while feldspars, (10–25%), calcite (5–10%) and phyllosilicates (<5%, mostly chlorite and muscovite) appear in smaller amounts.

It is important to point out that although the church is very near the sea, and therefore exposed to the deposit of marine aerosols, no traces of sodium chloride or other soluble salts in the sandstone have been detected using XRD analysis. In order to overcome possible limitations of this technique in the detection of salt phases in very low concentrations, we decided to try to extract NaCl using distilled water. We used conductimetry to measure the concentration of salt in solution. For this purpose we prepared a series of NaCl solutions with known concentrations which we used as a standard for the calibration of the conductimetry apparatus.

Conductimetric analysis of the sandstones from the quarry (which were further away from the coast than the church and therefore less exposed to salt deposits from marine aerosols) showed NaCl concentration levels of 0.07 wt.%, whereas samples from the church ranged from 0.04 to 0.21 wt.%. These figures indicate that a small amount of NaCl accumulated in certain areas of the building, although this never exceeded 0.21 wt.%. However, salt crystallization as a direct cause of damage seems improbable because of the relatively low amounts of salts detected.

In all the samples from the quarry and from the church, we observed a concentration of carbonates of around 10 wt.%. They were dissolved in dilute acetic acid solution and not counted in granulometric fractions. The stone from the quarry is almost identical to that from the building. The clay fraction amounts to average values of 7 wt.% which are very similar to those for the silt fraction (around 5 wt.%). The sand fraction is the largest with average figures of 88 wt.%.

XRD results indicate that the main mineral in the clay and silt fractions from both the church and the quarry is a mixed layer clay (probably corrensite according to the nomenclature proposed by Bailey [43]), made up of at least two different types of layers, chlorite and smectite, both with d_{001} of approximately 14 Å. The presence of mixed layer clays was confirmed by the appearance of reflections at 28 and 14 Å (Fig. 3). When heated to 550 °C a broad reflection at ~12 Å appeared, confirming the regular nature of the interstratified clay. Furthermore, it was shown that the d-spacing for one of these layers changed to 10 Å (smectitic layer), while the other (chlorite layer) remained at 14 Å. After treatments with EG and DMSO the d_{001} and d_{002} values remained at 28 Å and 14 Å, respectively, or they expanded slightly, as can clearly be observed in the displacement of the diffraction line at 7.13 Å with EG or at 29.4 Å with DMSO treatment which confirms the presence of a swelling clay mineral (smectite) in the mixed

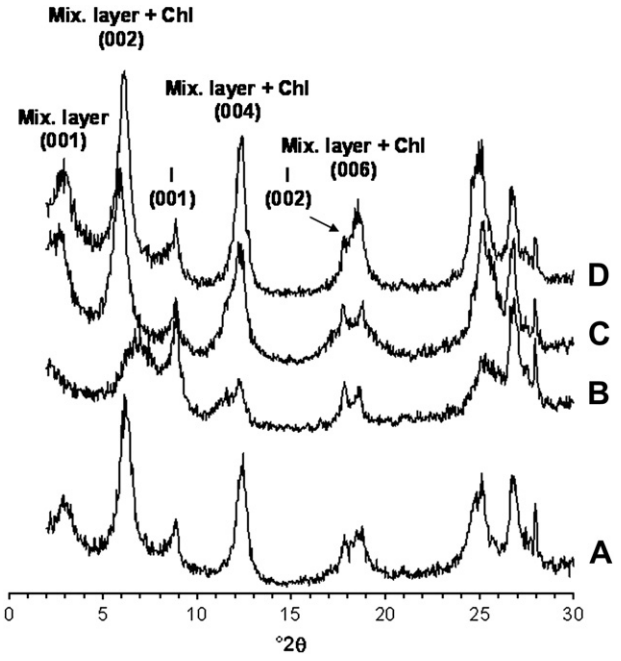

Fig. 3. Diffractograms of the clay fraction from the untreated sandstone (A), heated to 550 °C (B), treated with ethylene-glycol (C) and dimethyl-sulphoxide (D). Mix. layer, mixed layer smectite-chlorite; Sm, smectite; Chl, chlorite; Ill, Illite.

layer (Fig. 3). Illite was identified by a diffraction line at 10 Å which does not change with any of the treatments. We also identified small amounts of chlorite and the presence of kaolinite cannot be discarded (Fig. 3). The only difference between the silt and clay fractions was that small amounts of quartz were found in the silt fraction. No significant mineralogical differences were detected between the grey and brown varieties of sandstone. However, it seems that chlorite shows higher levels of decay in brown sandstone which is evidenced by a broadening of the diffraction peaks caused by a reduction in the crystallinity. This decay is commonly associated with the presence of Fe in the structure. Furthermore, Fe can be released and oxidized and gives the host material a slightly reddish-brown colour.

3.2. Texture

Due to the high concentration of quartz and smaller amounts of feldspars and other lithic fragments (Fig. 4a), the sandstone can be classified in petrological terms as arkose [44]. The quartz crystals are angular to subrounded in shape. They are surrounded by feldspars (partially altered to sericite), phyllosilicates and interparticle calcareous matrix that appears in sparse, unevenly distributed amounts. Quartz, feldspar and some phyllosilicate crystals are around 350 μm in size (Fig. 4b). No bioclasts were observed and some macropores can be recognized.

The phyllosilicates basal planes are normally placed parallel to the stratification planes. Fractures can appear parallel to these planes and are manifested macroscopically in the form of scaling and flakes. In some cases quartz- and feldspar-rich layers can be identified alternating with other layers rich in phyllosilicates.

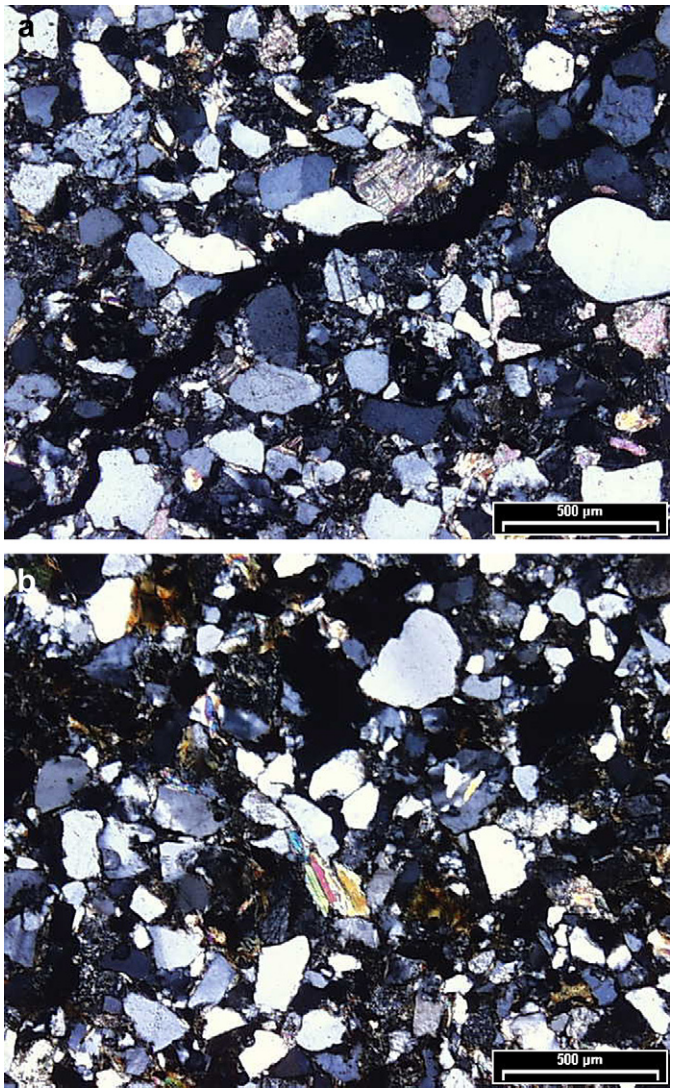

Fig. 4. Optical microscope images of the sandstones (crossed nicols). (a) Crack development in the sandstone from the monument; quartz and feldspar crystals are recognizable. (b) General view of a sandstone sample from the quarry where muscovite sheets and a high concentration of quartz crystals can be identified.

As mentioned previously, the samples from the quarry, both grey and brown stone, have similar composition and texture to those from the monument. However, unlike the samples from the monument, quarry samples do not contain fractures.

Under the SEM it is possible to observe subangular grains of quartz and feldspar (the latter showing signs of alteration) surrounded by a clay matrix (Fig. 5a). Clay minerals of up to several micrometres in size appear which are flat in shape, like small flakes or curled leaves piled up according to their (001) basal planes (Fig. 5b). These curled-leaf shapes are typical of smectites [20,45].

3.3. Dynamic parameters

Table 1 shows the results of ultrasound analysis of the two varieties of sandstone (grey and brown) sampled from the quarry. The brown variety shows slightly lower V_P values

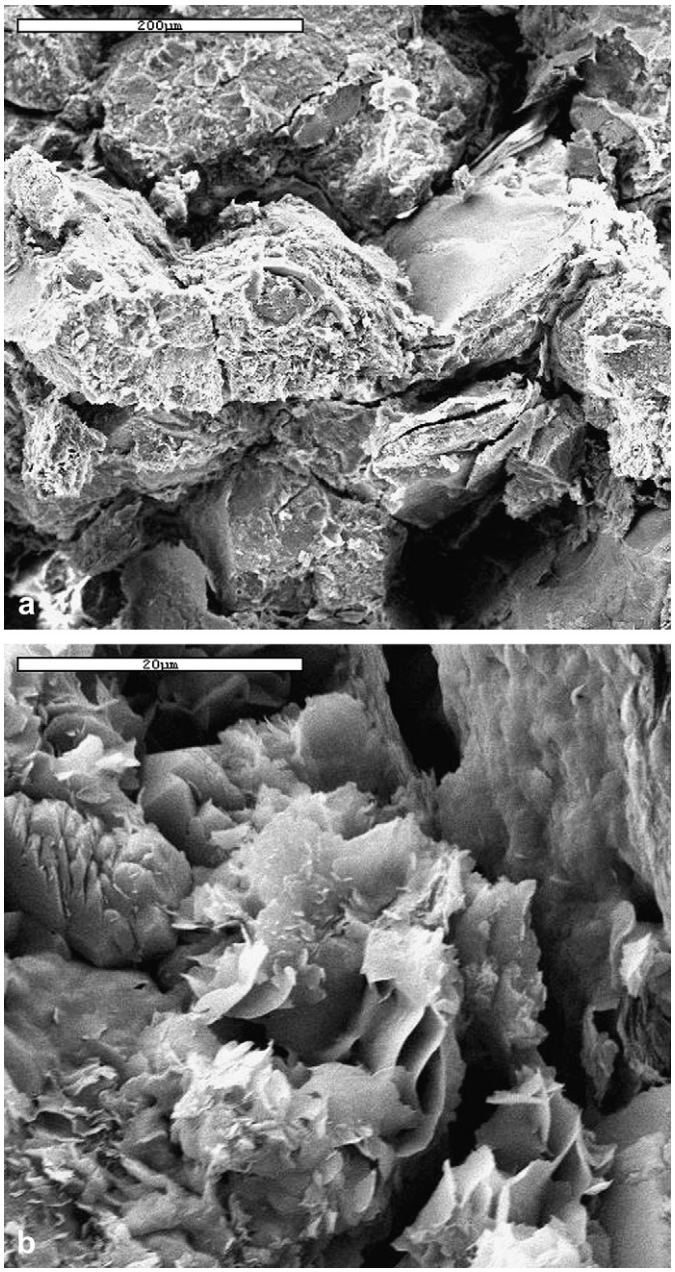

Fig. 5. SEM photomicrographs of the sandstone. (a) Interparticle position of the clay minerals. (b) Curled-leaf shape of smectites.

than the grey variety, which could imply lower mechanical resistance.

It is important to note that the sandstones show an extremely high total anisotropy (ΔM). This is because of their very marked bedding planes and because of the orientation of the crystals (mostly phyllosilicates) previously observed under optical and SEM microscopes.

This marked anisotropy is accentuated due to the fact that the clays lie flat in a parallel position to the bedding planes. In these conditions we would expect flakes to form during wet/dry cycles, as clays are very sensitive to this kind of change [13,46]. Therefore, it is possible for these flakes to break off or become detached along these planes of weakness as can be seen in the sandstone from the building.

Table 1
Average velocities for the propagation of ultrasonic V_P pulses (in m/s) and values for total anisotropy (ΔM, in %) in the sandstone samples from the quarry

	V_{P1}	V_{P2}	V_{P3}	ΔM
Grey	2123 ± 136	3100 ± 119	2765 ± 135	27.6 ± 2.8
Brown	2039 ± 68	2935 ± 94	2853 ± 73	29.5 ± 1.4

3.4. Hydric properties

In order to understand the alterability of building materials it is essential to determine the speed and the amount of water that penetrates and leaves the porous system [38,47]. Fig. 6 shows the absorption/desorption curves for the two sandstone varieties found in Tarifa that show quite similar behaviour. In just 24 h the samples are almost saturated with water. The brown sandstone absorbs slightly more water (see values for A_b and A_f, Table 2), a fact that may suggest a greater susceptibility to decay of these samples as we have shown before. Given their low porosity (Pa), the amount of water absorbed is small (around 4%).

It is important to point out that grey and brown sandstones show only very slight variations in porosity between the different blocks of stone. Table 2 shows that the grey variety of sandstone is less porous than the brown one.

The drying behaviour of the two stone types is very similar, as can be seen in the drying index data (Di, Table 2). It is important to stress that the first stage of drying, in which weight loss is linear against time (“constant rate period” [48]) is quite short (it lasts about 10 h). However, the stage of drying due to transfer of water vapour from inside the pores to the surface of the samples (“falling rate period” [48]) is relatively long (several days). This suggests that the phenomenon of clay swelling and/or dissolving of the carbonated cement may be significant. However the drying time, in absolute terms, is not excessively long, which indicates that the wet-dry cycles may easily occur

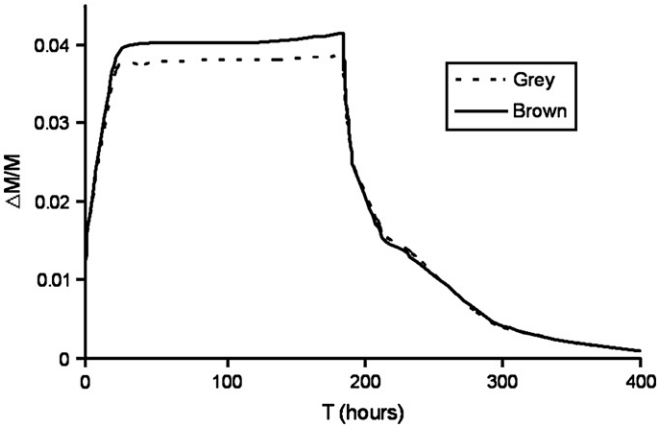

Fig. 6. Weight change due to absorption and drying of the grey (discontinuous line) and brown sandstone (continuous line) vs. time (in hours).

Table 2
Average hydric parameters for the sandstones from the quarry after absorption-drying tests

	Grey	Brown
A_b	3.82 ± 0.09	4.09 ± 0.46
A_f	3.87 ± 0.10	4.15 ± 0.48
Ca ($\times 10^{-2}$)	0.15 ± 0.01	0.16 ± 0.03
Di	0.66 ± 0.01	0.64 ± 0.01
Pa	8.48 ± 0.86	11.18 ± 0.21
ρ_a	2.44 ± 0.01	2.39 ± 0.05
ρ_r	2.70 ± 0.01	2.65 ± 0.03

A_b, absorption (%); A_f, absorption under vacuum (%); Ca, Absorption coefficient; Di, drying index; Pa, open porosity (%); ρ_a, apparent density (g/cm^3); ρ_r, real density (g/cm^3).

in a short period of time for example on a daily basis, something that results quite devastating for this type of stone.

The capillary rise tests (Fig. 7) confirmed the anisotropic nature of the sandstones previously observed with ultrasound analysis. In both varieties of stone absorption speed and amount of water absorbed is lower in the direction perpendicular to the stratification (Face 1) when compared to the directions parallel to the bedding planes (Faces 2 and 3). In addition, comparing the graphs for the brown and the grey stone, the latter shows a smaller variation in weight ($W(t)/S$) between the curve for Face 1 and the curves for Faces 2 and 3. These results suggest that the bedding planes are more highly developed in the brown sandstone due to a clear concentration of phyllosilicates/clay minerals along these planes. This leads to higher levels of anisotropy, something that is congruent with the higher ΔM value in this variety (Table 1).

The capillary rise (Fig. 7) is relatively low. These results show that, once the water is in contact with the sandstone it only penetrates the most superficial areas of the rock, namely the first few centimetres below the surface. This means that between the wet area and the dry inner part, a discontinuity is created in which mechanical stress phenomena can occur. Such stress phenomena will contribute to the development of fracture planes parallel to the surface, especially in blocks that are laid with the bedding planes parallel to the exposed face. This type of behaviour explains why contour-scaling is such a widespread problem in this building. On the other hand, cracks normal to the exposed surface will develop upon drying, as observed on different areas of the building.

3.5. The porous system

Table 3 shows the results of the MIP porometric analysis of samples from both the church and the quarry. Note how P, ρ_a and ρ_r values measured with this technique are somewhat different compared to those of hydric tests (Table 2). However, this seems reasonable given that we are considering liquids (water and mercury) with dissimilar physical properties. Porosities measured after MIP analyses might be higher than those calculated from hydric test results [38].

The samples from the quarry show higher porosity values in brown sandstone (up to about 15%) than in grey (less than 10%), confirming the results obtained in hydric tests. The pore access size distribution is polymodal in the material from the quarry with distribution maxima at around 0.02, 0.5 and 100 μm, with the main group being those of 0.5 μm (Fig. 8), i.e. pores with radius less than 1 μm.

Both varieties show a similar fraction of micro-mesoporosity, which is typically related to the clay mineral fraction [49]. The pore volume fraction obtained with nitrogen adsorption was 0.011 cm^3/g for the brown stone and 0.007 cm^3/g for the grey (Fig. 8). We should point out that in terms of pore distribution the two samples of grey stone (from the church and from the quarry) are more similar than the brown stone samples.

We observed that the damaged materials (from the church) showed substantially higher porosity values than those from the quarry. The average porosity values for the samples from the church were 15–20% higher than those from the quarry.

Regarding the pore access size distribution, the most striking feature is the appearance of a third type of pores with an access radius between 10 and 50 μm in the damaged samples (Fig. 8).

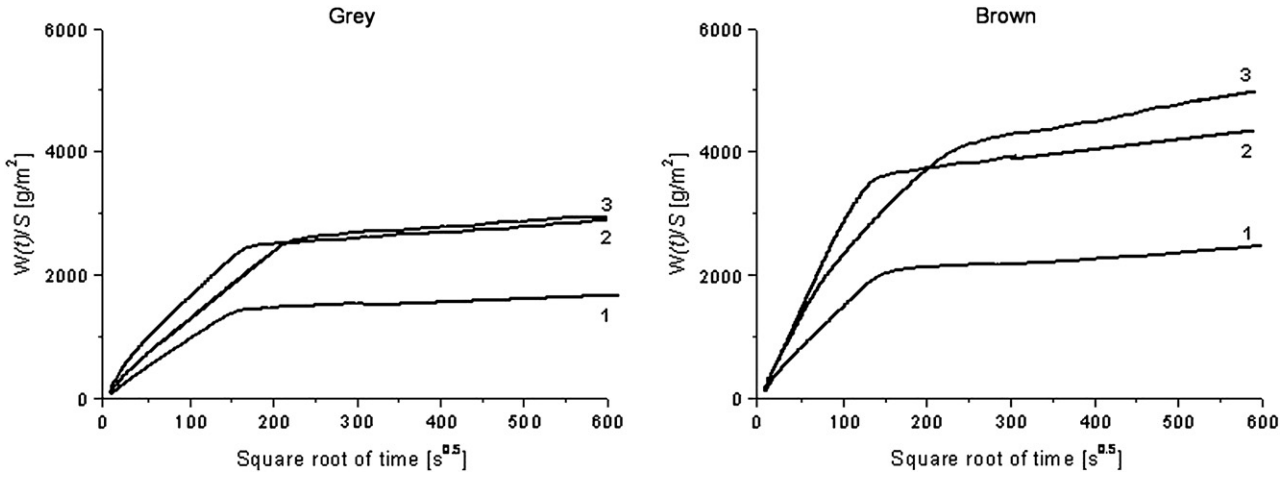

Fig. 7. Capillarity curves of the sandstone (weight change vs. time in hours). Face 1, direction of propagation of the water perpendicular to the bedding planes; Faces 2 and 3, direction of propagation of the water parallel to the bedding planes.

Table 3
Average results of the porometric analysis (Hg porosimetry) of the sandstone from the building (T) and from the quarry (TC)

	Sample	S	ρ_a	ρ_r	P
Grey	T	5.85 ± 0.66	2.21 ± 0.04	2.50 ± 0.02	11.48 ± 1.23
Brown	T	6.53 ± 0.48	2.09 ± 0.07	2.51 ± 0.02	16.70 ± 3.10
Grey	TC	6.05 ± 0.76	2.28 ± 0.01	2.52 ± 0.01	9.49 ± 0.67
Brown	TC	6.96 ± 0.39	2.15 ± 0.09	2.51 ± 0.01	14.54 ± 3.26

S, surface area (m^2/g); ρ_a, apparent density (g/cm^3); ρ_r, real density (g/cm^3); P, porosity (%).

These pores correspond to both fissures that appear in flaking areas, and pores created by the dissolving of calcareous cement.

The new family of pores (those measuring between 10 and 50 μm) facilitates the penetration of fluids (gases and liquids) into the rock, and thus, conditions its behaviour with respect to most of the damage mechanisms in which water is involved [50]. Moreover, the increase in porosity (P, Table 3) contributes directly to the poor mechanical behaviour of the rock [51].

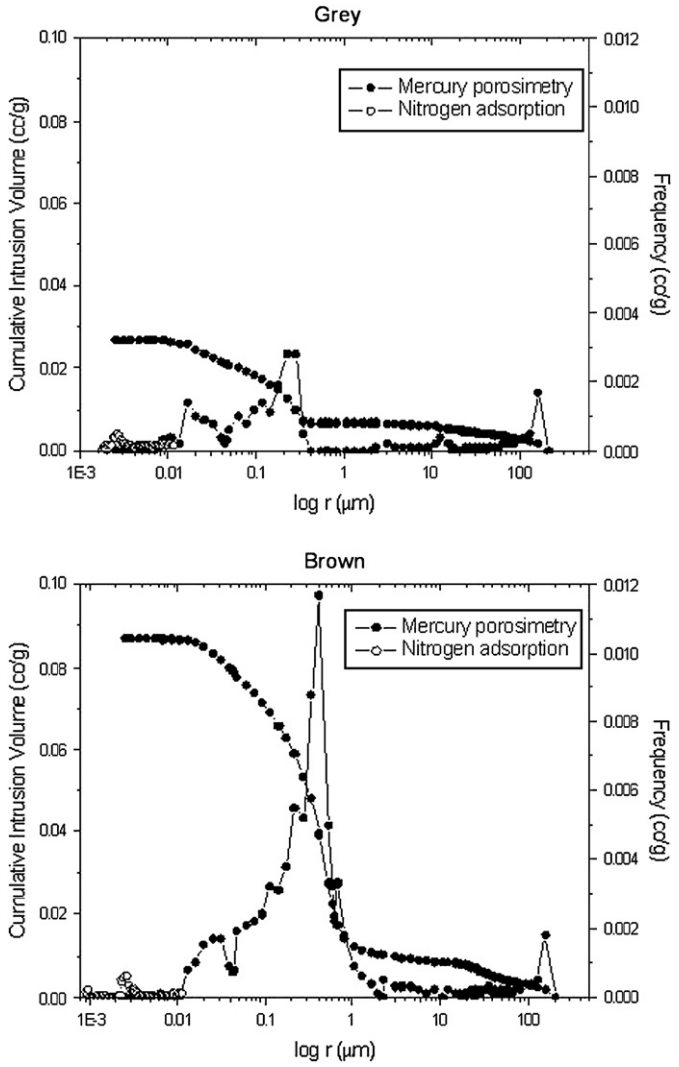

Fig. 8. Cumulative mercury intrusion curves and pore size distribution curves obtained by nitrogen adsorption and mercury intrusion porosimetry for the brown and grey varieties of sandstone.

3.6. Hydric expansion

During the test the sandstone samples were partially saturated, thus, the water moved through the rock by capillary forces. Fig. 9 shows that the brown sandstone ($\Delta l/l_0 \sim 0.004$ mm/mm) expands about 10 times more than the grey ($\Delta l/l_0 \sim 0.0004$ mm/mm). This is due to the textural differences between the two varieties: the brown sandstone is more porous than the grey, allowing for larger amounts of water to interact with the minerals that make up the rock (in particular the expansive mixed layer clays); the swelling minerals in the brown sandstone tend to be located in the bedding planes, something uncommon in the case of the grey sandstone which has a similar concentration of clays, however, more evenly distributed within the rock. The concentration of the clay minerals along the bedding planes leads to a higher capillary suction speed in the brown sandstone, especially in directions parallel to the bedding planes (Fig. 7). These characteristics result in a lower mechanical resistance, which we had deduced from its dynamic behaviour (V_P values, Table 1). The brown sandstone will be, therefore, more susceptible to decay caused by water-related expansion-contraction cycles than the grey stone.

4. Discussion and conclusions

The Tarifa sandstone is a relatively non-porous stone; however, the majority of the pores are very small (less than 1 μm) and it can therefore be classified as a microporous stone according to the classification proposed by Esbert et al. [38]. Experiments have shown that rocks with a high volume of pores with a radius of <1 μm are easily affected by salt crystallization or by freeze–thawing [52]. However, freeze-thawing is not an issue in Tarifa [53], and salts appear in very low concentrations. Thus, the main decay phenomena to which the stone in this building is subjected are processes of physical alteration which cause the development of fissures or fractures,

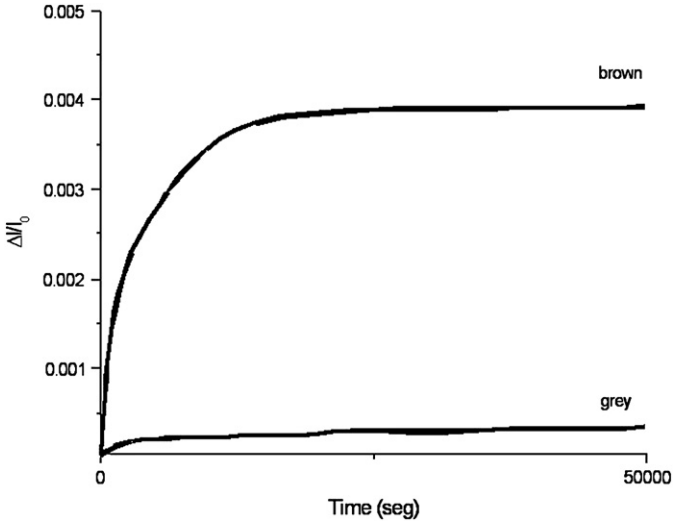

Fig. 9. Kinetics of relative hydric expansion ($\Delta l/l_0$) during the rise of water by capillarity.

normally parallel to the exposed face of the stone. The appearance of pores and/or fissures with an access size between 10 and 50 μm result in a significant increase in the open porosity and in a general mechanical weakening of the stone (which means that the decay process will continue at an ever-increasing rate). The main decay mechanism is the swelling (or expansion) and shrinking of the clay minerals that form the cement or the matrix of the sandstone. XRD data revealed that there are mixed layer clays made up of chlorite and smectite. In the presence of water the latter may undergo intracrystalline swelling. In addition all clay minerals, including chlorite + illite, may be subjected to osmotic-type swelling processes, if the pores in the rock contain an electrolyte in solution [54]. NaCl is one of the most effective electrolytes in osmotic swelling of clays [55], and this salt has been found in the sandstone, albeit in very small amounts. Fig. 10 shows the processes of intracrystalline and osmotic swelling in clays: (a) solely the ''smectite type'' suffers intracrystalline swelling, increasing the basal spacing d ($d_2 > d_1$) as the ions (in this case Na ions) situated in the interlayer are hydrated; (b) particles from any type of clay subjected to processes of osmotic swelling due to differences in the concentration of Na ions between the clay particles and the pores in the rock ($C_1 >> C_2$). In order to even out these concentration differences ($C_1 \rightarrow C_2$) water enters the pore space between particles and separates them due to osmotic expansion.

Sodium chloride, instead of causing decay by inducing salt crystallization pressure in the pores of the sandstone, as has been reported for similar materials [53], seems to play here a significant role in the swelling processes undergone by the clays. The salt reaches the building in the form of sea spray, a very common phenomenon in this coastal area that is almost constantly buffeted by strong East and West winds.

The hydric behaviour of the sandstone favours the capillary absorption of water to depths of up to 1–2 cm inside the rock. This means that when condensation occurs (normally every night) or when rain falls directly on the walls (wind-driven rain), the first few centimetres of the rock may experience a volume increase (the clays expand) creating an area of tension (with the resulting development of fractures) between the wet zone of the stone and the dry zone behind it. Swelling stresses lead to the development of scales and flakes as well as contour-scaling. Once the external wet layer has dried (evaporation due to the action of the sun, temperature increase during the day, and/or evaporation accelerated by the effects of the wind), the clays contract causing the appearance of drying or retraction fractures perpendicular to the surface as observed all over the façade of the church.

It is important to point out that the flaking and scaling processes are very closely related to the structural anisotropy of the stone. Studies carried out with optical microscopy and ultrasound analysis as well as the capillarity rise test have shown that this type of sandstone has a very pronounced orientation of the phyllosilicates which are oriented with their basal planes parallel to the original sedimentation beds. These planes are particularly sensitive to flaking and/or scaling, as they act as planes of weakness. This characteristic is more pronounced in the case of the brown sandstone because it suffers greater hydric swelling due to its higher porosity and the concentration of phyllosilicates in the bedding planes. This variety also shows lower mechanical resistance than the grey stone, something which can be deduced from the velocity of the ultrasonic waves (V_P, Table 1). Thus, the brown sandstone will be less resistant towards mechanical action of hydric expansion-contraction processes as can be observed in the building where it decays at a faster rate than the grey variety.

In conclusion, the interaction of the following variables, i.e. water, swelling clays and NaCl, together with the high degree of anisotropy of this building stone, causes severe decay problems to the building. The most effective strategy for the conservation of this material would therefore be controlling these variables to minimize or prevent future decay and damage to the stone. This conservation strategy must above all seek to prevent the water from penetrating into the pores in the rock by implementing barriers (e.g. hydrophobic coatings), reduce the amount of NaCl in the pores for example by poulticing and increase the mechanical resistance of the sandstone in areas of severe decay using suitable consolidants.

The results we have obtained make an important contribution to the study of decay of sandstone in historic buildings, and may facilitate the choice of the most suitable restoration method for the Church of San Mateo in Tarifa.

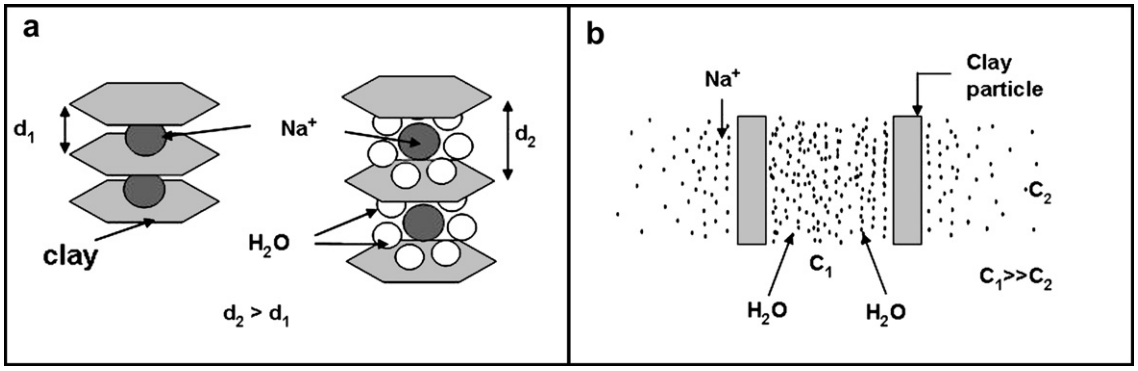

Fig. 10. Diagram of the processes of intracrystalline swelling (a) and osmotic swelling (b) of the clays. d, basal spacing of the clays; C, concentration of Na ions. Modified from Madsen and Müller Vonmoos [56].

Acknowledgements

This research has been supported by the Research Projects MEC MAT2003-02723, MAT2004-6804 and GV05/129 and by the Research Groups of Junta de Andalucía RNM 179 and Generalitat Valenciana 03/158. We thank Nigel Walkington for the translation of the manuscript.

References

[1] J.M. Cabrera Garrido, Causas de alteración y métodos de conservación aplicables a los monumentos hechos en piedra, Materiales de Construcción 174 (1979) 1–38.
[2] G. Cultrone, E. Sebastián, M. Ortega Huertas, Durability of masonry systems: a laboratory study, Construction and Building Materials 21 (2007) 40–51.
[3] C.A. Price, Stone Conservation. An Overview of Current Research, Getty Conservation Institute, Los Angeles, 1996.
[4] J. Simão, E. Ruiz Agudo, C. Rodriguez-Navarro, Effects of particulate matter from gasoline and diesel vehicle exhaust emissions on silicate stones sulfation, Atmospheric Environment 40 (2006) 6905–6917.
[5] T.T. Ngoc Lan, R. Nishimura, Y. Tsujino, Y. Satoh, N.T. Phuong Thoa, M. Yokoi, Y. Maeda, The effects of air pollution and climatic factors on atmospheric corrosion of marble under field exposure, Corrosion Science 47 (2005) 1023–1038.
[6] J.W. Morse, R.S. Arvidson, The dissolution kinetics of major sedimentary carbonate minerals, Earth-Science Reviews 58 (2002) 51–84.
[7] A. Moropoulou, K. Bisbikou, K. Torfs, R. Van Grieken, F. Zezza, F. Macri, Origin and growth of weathering crusts on ancient marbles in industrial atmosphere, Atmospheric Environment 32 (1998) 967–982.
[8] E.M. Winkler, Weathering and weathering rates of natural stone, Environmental Geology 9 (1987) 85–92.
[9] D. Benavente, M.A. García del Cura, J. García Guinea, S. Sanchez Moral, S. Ordóñez, Role of pore structure in salt crystallisation in unsaturated porous stone, Journal of Crystal Growth 260 (2004) 532–544.
[10] G. Caneva, M.P. Nugari, O. Salvadori, La Biologia nel Restauro, Nardini, Firenze, 1994.
[11] R. Snethlage, E. Wendler, Moisture cycles and sandstone degradation, in: N.S. Baer, R. Snethlage (Eds.), Saving our Architectural Heritage: The conservation of Historic Stone Structures, John Wiley & Sons Ltd., Chichester, 1997, pp. 7–24.
[12] K. Hall, A. Hall, Weathering by wetting and drying: some experimental results, Earth Surface Processes and Landforms 21 (1996) 365–376.
[13] J. Delgado Rodrigues, Evaluación del comportamiento expansivo de las rocas y su interés en conservación, Materiales de Construcción 51 (2001) 183–195.
[14] Zehnder, K., Weathering of molasses sandstones on monuments and natural outcrops, 3rd International Congress on the Deterioration and Preservation of Stone, Venice, 24–27 October, 1979, pp. 91–105.
[15] I. Jiménez González, G.W. Scherer, Effect of swelling inhibitors on the swelling and stress relaxation of clay bearing stones, Environmental Geology 46 (2004) 364–377.
[16] B. Fitzner, K. Heinrichs, Weathering forms and rock characteristics of historical monuments carved from bedrocks in Petra/Jordan, in: N.S. Baer, C. Sabbioni, A.I. Sors (Eds.), Proceedings of the European Symposium "Science, Technology and European Cultural Heritage", Bologna (Italy), 13–16 June, Buttherworth-Heinemann, Oxford, 1989, pp. 908–911.
[17] C. Félix, V. Furlan, Variations dimensionnelles des gres et calcaires liees a leur consolidation avec un silicate d'ethyle, in: V. Fassina (Ed.), 3rd International Symposium on the Conservation of Monuments in the Mediterranean Basin (1994), pp. 288–295 Venice.
[18] F. Veniale, M. Setti, C. Rodriguez-Navarro, S. Lodola, Role of clay constituents in stone decay processes, Materiales de Construcción 51 (2001) 163–182.
[19] J.R. Dunn, P.P. Hudec, Water, clay and rock soundness, Ohio Journal of Science 66 (1966) 153–168.
[20] J.C. Backer, P.J.R. Uwins, I.D.R. Mackinnon, ESEM study of illite/smectite freshwater sensitivity in sandstone reservoirs, Journal of Petroleum Science and Engineering 9 (1993) 83–94.
[21] M.T. Martin Patino, F. Madruga, J. Saavedra, The internal structure of the Villamayor sandstone as it affects its use as a construction material, Applied Clay Science 8 (1993) 61–77.
[22] C. Felix, Sandstone linear swelling due to isothermal water sorption, in: F.H. Wittmann (Ed.), International Congress on Material Science and Restoration, Technische Akademie Esslingen, Ostfildern, 1983, pp. 305–310.
[23] UNI 11182, Beni culturali—Materiali lapidei naturali ed artificiali—Descrizione della forma di alterazione—Termini e definizioni, Roma, 2006.
[24] B. Fitzner, K. Heinrichs, Damage diagnosis on stone monuments—weathering forms, damage categories and damage indices, in: R. Prikryl, H.A. Viles (Eds.), Proceedings of the International Conference "Stone Weathering and Atmospheric Pollution Network (SWAPNET)" Understanding and Managing Stone Decay, Karolinum Press, Prague, 2002, pp. 11–56.
[25] P. Rodríguez Jiménez, M.D. Ruiz Cruz, Mineralogía y génesis de las arcillas de las Unidades del Campo de Gibraltar. V. Unidad de Bolonia, Estudios Geológicos 46 (1990) 3–14.
[26] M.D. Ruiz Cruz, Clay mineral assemblages in flysch from the Campo de Gibraltar area (Spain), Clay Minerals 34 (1999) 345–364.
[27] M.D. Ruiz Cruz, M. Esteras Martín, Caracterización geoquímica de la esmectita en varias formaciones arcillosas de los flyschs del Campo de Gibraltar (Cádiz, España), Estudios Geológicos 49 (1993) 287–294.
[28] M. Ortega Huertas, M. Sebastián Pardo, M. Rodríguez Gallego, F. López Aguayo, Mineralogía de arcillas en sedimentos turbidíticos de las unidades del Campo de Gibraltar (Cádiz), Tecniterrae 51 (1983) 43–48.
[29] J.D. Martín Ramos, XPowder, a software package for powder X-ray diffraction analysis, Legal Deposit GR 1001/04 (2004) Further information about this software is available at, http://xpowder.com web page.
[30] H. Chamley, Clay Sedimentology, Springer, Berlin, 1989.
[31] G. Brunton, Vapour pressure glycolation of oriented clay minerals, American Mineralogist 40 (1955) 124–126.
[32] F. González García, M. Sánchez Camazano, Differentiation of kaolinite from chlorite by treatment with dimethylsulfoxide, Clay Minerals 7 (1968) 447–450.
[33] D.M. Moore, R.C. Reynolds, X-Ray Diffraction and the Identification and Analysis of Clay Minerals, Oxford University Press, Oxford, 1989.
[34] ASTM D 2845, Standard test method for laboratory determination of pulse velocities and ultrasonic elastic constants of rock, American Society for Testing and Materials, West Conshohocken (USA), 1983.
[35] J. Guydader, A. Denis, Propagation des ondes dans les roches anisotropes sous contrainte évaluation de la qualité des schistes ardoisiers, Bulletin of Engineering Geology 33 (1986) 49–55.
[36] UNI EN 13755, Metodi di prova per pietre naturali—Determinazione dell'assorbimento d'acqua a pressione atmosferica, Roma, 2002.
[37] G. Cultrone, E. Sebastián, K. Elert, M.J. de la Torre, O. Cazalla, C. Rodriguez-Navarro, Influence of mineralogy and firing temperature on porosity of bricks, Journal of The European Ceramic Society 24 (2004) 247–564.
[38] R.M. Esbert, J. Ordaz, F.J. Alonso, M. Montoto, T. González Limón, M. Álvarez de Buergo Ballester, Manual de diagnosis y tratamiento de materiales pétreos y cerámicos, Collegi d'Apparelladors i Arquitectes Tècnics de Barcelona, Barcelona, 1997.
[39] NORMAL 29/88, Misura dell'indice di asciugamento (drying index), CNR-ICR, Roma, 1988.
[40] D. Benavente, N. Cueto, J. Martínez Martínez, M.A. García del Cura, J.C. Cañaveras, Influence of petrophysical properties on the salt weathering of porous building rocks, Environmental Geology 52 (2007) 197–206.
[41] UNI EN 1936, Metodi di prova per pietre naturali—Determinazione delle masse volumiche reale e apparente e della porositá totale aperta, Roma, 2007.

[42] UNI EN 1925, Metodi di prova per pietre naturali—Determinazione del coefficiente di assorbimento d'acqua per capillarità, Roma, 2000.
[43] S.W. Bailey, Nomenclature for regular interstratifications, AIPEA Nomenclature Committee, Louvain (Belgium), 1982.
[44] R.L. Folk, Petrology of Sedimentary Rocks, Hemphill Publishing, Austin, TX, 1974.
[45] C. Viseras Iborra, G. Cultrone, P. Cerezo, C. Aguzzi, M.T. Baschini, J. Vallés, A. López Galindo, Characterisation of northern Patagonian bentonites for pharmaceutical uses, Applied Clay Science 31 (2006) 272–281.
[46] C. Rodriguez-Navarro, E. Sebastián, E. Doehne, W.S. Ginell, The role of sepiolite-palygorskite in the decay of ancient Egyptian limestone sculptures, Clays and Clay Minerals 46 (1998) 414–422.
[47] A.E. Charola, L. Lazzarini, Material degradation caused by acid rain, in: R. Baboian (Ed.), ACS Symposium Series no. 318, American Chemical Society, Washington, 1986, pp. 250–258.
[48] G.W. Scherer, Theory of drying, Journal of the American Ceramic Society 73 (1990) 3–14.
[49] F. Rouquerol, J. Rouquerol, K. Sing, Adsorption by Powders and Porous Solids: Principles, Methodology and Applications, Academic Press, San Diego, 1999.
[50] W.C. Kowalski, L'influence des variations de teneur en eau sur la resistance mécanique et la déformation des roches dans la zone d'altération, Bulletin de l'Association Internationale de Geologie de l'Ingenieur 12 (1975) 37–43.
[51] L.I. González del Vallejo, M. Ferrer, L. Ortuño, C. Oteo, Ingeniería Geológica, Prentice Hall, Madrid, 2002.
[52] S. Ordóñez, R. Fort, M.A. Garía del Cura, Pore size distribution and the durability of a porous limestone, Quarterly Journal of Engineering Geology 30 (1997) 221–230.
[53] M. Hoyos, S. Sánchez Moral, E. Sanz Rubio, J.C. Cañaveras, Causas y mecanismos de deterioro de los materiales pétreos del pavimento del conjunto arqueológico de Baelo Claudia, Cádiz/España, Materiales de Construcción 49 (1999) 5–18.
[54] C. Rodriguez-Navarro, E. Hansen, E. Sebastián, W.S. Ginell, The role of clays in the decay of ancient Egyptian limestone sculptures, Journal of the American Institute for Conservation 36 (1997) 151–163.
[55] K.E. Schmittner, P. Giresse, The impact of atmospheric sodium on erodibility of clay in a coastal Mediterranean region, Environmental Geology 37 (1999) 195–206.
[56] F.T. Madsen, M. Müller Vonmoos, The swelling behaviour of clays, Applied Clay Science 4 (1989) 143–156.